

ECONOMIC GEOLOGY

AND THE

BULLETIN OF THE SOCIETY OF ECONOMIC GEOLOGISTS

VOL. 89

JUNE-JULY, 1994

No. 4

Gold Mineralization and Fault Evolution at the Dixie Comstock Mine, Churchill County, Nevada

PETER G. VIKRE

ASARCO Incorporated, 510 East Plumb Lane, Reno, Nevada 89502

Abstract

Gold ore at the Dixie Comstock mine, Churchill County, Nevada, is composed of quartz breccia, quartz stockwork, incipiently crushed gabbro, and minor fault gouge. The ore zone forms a mullion within a range-bounding normal fault, the Dixie Comstock mine fault, which originated in the middle Miocene and separates Jurassic gabbro and Tertiary volcanic rocks of the Stillwater Range to the west from Quaternary colluvium of Dixie Valley to the east. Within the mullion, a potentially bulk mineable resource of several million tons grading ~ 0.06 oz of gold per ton has been defined by drilling.

Within the fault zone, clasts of gabbro in quartz breccia, quartz stockwork gabbro, and incipiently crushed gabbro are altered to quartz, sericite, chlorite, montmorillonite, and sulfides. Gold occurs as electrum in quartz that cements quartz breccia, in quartz stockwork veins with quartz, pyrite, chalcopyrite, and montmorillonite in breccia clasts, and in veins in incipiently crushed gabbro. Fluid inclusion microthermometry and stable isotope analyses of mineralized quartz matrix and two later stages of quartz and calcite show that ore fluid was 180°C , near-boiling meteoric water.

An inverse stratigraphy of thermal spring silica detritus in hanging-wall colluvium, microthermometry and isotopic compositions of fluid inclusion water from quartz breccia, a subjacent geothermal reservoir, and radiometric ages of hydrothermal minerals in the fault cumulatively support a mid-Pleistocene age for gold mineralization. The lower average displacement rate on the Dixie Comstock mine fault that is required by the age and thickness of eroded thermal spring sinter and underlying quartz breccia and stockwork, compared to higher recent displacement rates along range-bounding faults on the western side of Dixie Valley, suggests that the current pattern of temporal clustering of fault displacements began by the mid-Pleistocene.

Introduction

THE Dixie Comstock gold mine is situated on the eastern margin of the Stillwater Range, Churchill County, Nevada, about 110 mi east of Reno (Fig. 1). The range margin, which separates the Stillwater Range to the west from Dixie Valley to the east, is sharply curvilinear, locally very steep, and the site of several thermal springs and sinters associated with Pleistocene to historic Basin and Range faulting and geothermal resources (Wallace and Whitney, 1984; Hudson and Geissman, 1987, 1991; Slemmons and Bell, 1987; Waibel, 1987; Wallace, 1987; Bell and Katzer, 1990; Parry et al., 1991). The Basin and Range province of the western United States covers Nevada and parts of adjacent states and is characterized by thin crust, elevated heat flow, and active seis-

mic belts in addition to the pattern of north-south-aligned, alternating mountain ranges and valleys (Wallace, 1984; Oldow, 1992).

The mine was discovered in 1934 by panning drainages along the Stillwater Range margin. It produced an estimated 4,600 oz of gold from 10,000 tons of ore during intermittent operation from 1938 to 1970. Ore grades reportedly ranged from 0.5 to 3.0 oz Au/ton and small pockets of >15 oz Au/ton ore were mined; all production took place within 100 ft of the present surface (Vanderburg, 1940; W. Wilson, pers. commun., 1985; D. Hargrove, pers. commun., 1986). Mined ore consists of fault breccia of the Dixie Comstock mine fault that has been filled in and replaced to varying degrees by quartz, hereafter referred to as quartz breccia. Recent exploration has shown that most gold is confined to a mullion within

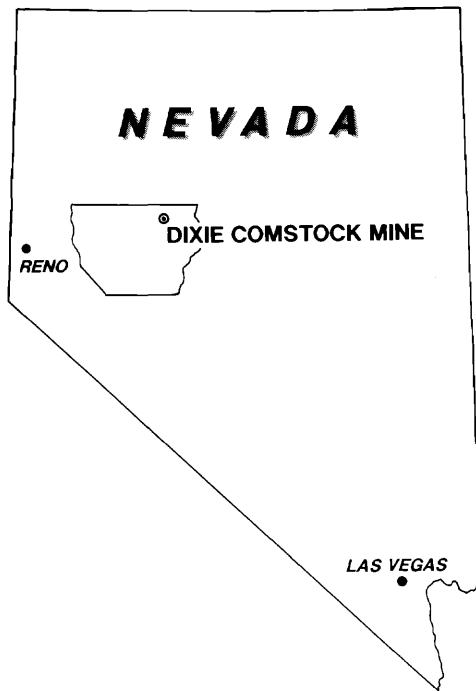


FIG. 1. Location map of the Dixie Comstock mine, Churchill County, Nevada.

the Dixie Comstock mine fault. Drilling by ASARCO Inc. in 1982 through 1984 defined an inventory of 1.8 million tons grading 0.058 oz Au/ton in the vicinity of old workings. Subsequent drilling of the same area by three other exploration companies resulted in similar resources.

This deposit is of geologic interest because of its close association with Basin and Range tectonism and geothermal activity, and proposed young age. The gold resource may be sufficiently voluminous to constitute a bulk deposit mineable by open pit.

Geology of the Mine Area

The Dixie Comstock mine fault separates footwall Jurassic and Tertiary rocks of the Stillwater Range from colluvium of Dixie Valley (Fig. 2). Jurassic rocks include coarse-grained hornblende gabbro and subordinate basalt, anorthosite, and albitite that compose the Humboldt lopolith (Page, 1965; Willden and Speed, 1974; Speed, 1976; Bell and Katzer, 1987). Along the steep scarp south from the mine is an alignment of small, irregular apophyses of an altered, granitic Cretaceous(?) intrusion (Table 1, sample DC89-5A) that contains quartz and pyrite stockwork veins in albitized carapaces (Fig. 2). Veins and lenses of calcite, barite, iron oxides, and copper sulfides in gabbro generally parallel the range margin and are associated with a colorful, sublinear array of light brown to white alteration zones that consist of quartz, albite, sericite, kaolinite, and iron oxide. Sev-

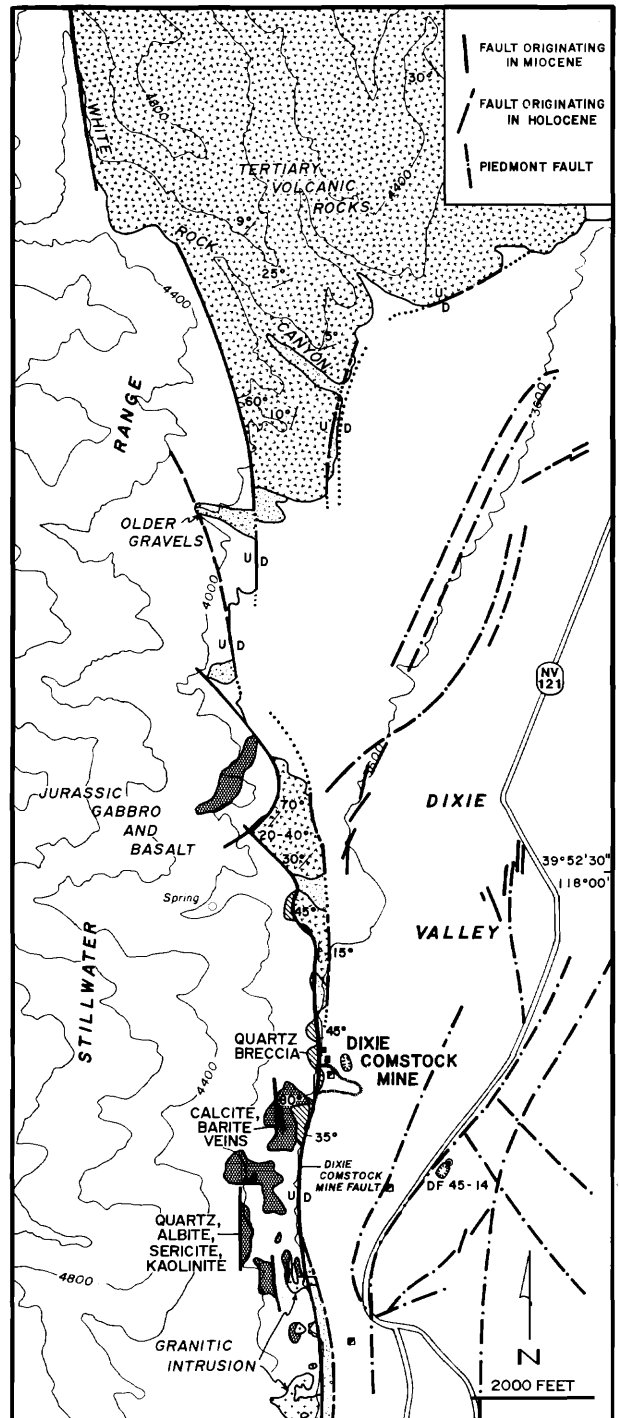


FIG. 2. Geologic map of the eastern Stillwater Range margin from the Dixie Comstock mine to White Rock Canyon. Dense dot patterns mark areas of quartz, albite, sericite, and kaolinite alteration of gabbro. Light dot pattern denotes terrace gravel deposits. Piedmont faults are interpreted from geophysical data and low-sun-angle photography (Bell et al., 1980). D = down, U = up.

eral of these alteration zones partially surround the granitic intrusion apophyses (Fig. 2) and all are probably related to them. The Late Cretaceous whole-rock

TABLE 1. Radiometric Ages of Altered Rocks, Albite, and Calcite in the Vicinity of the Dixie Comstock Mine

Sample no.	Location	Mineral or rock dated	% $\overline{\text{K}_2\text{O}}$	$^{40}\overline{\text{Ar}}$ moles/g	$^{40}\text{Ar}/\Sigma^{40}\text{Ar}\%$	Age (Ma)	Source
DC89-5A	1 mi S from Dixie Comstock mine portal	Albite from carapace of granitic intrusion	0.19	2.64495×10^{-11}	4.66	93.2 ± 7.8	1a
DC29-193	DDH, -193 ft, Dixie Comstock mine	Whole rock (altered gabbro)	1.08	1.1885×10^{-10}	62.6	74.9 ± 2.2	2
DC29-208.5	DDH, -208.5 ft, Dixie Comstock mine	Whole rock (sericitized gabbro)	6.24	1.354426×10^{-10}	65.2	15.0 ± 0.5	1a
DC29-210	DDH, -210 ft, Dixie Comstock mine	Whole rock (sericitized gabbro)	6.43	1.026935×10^{-10}	63.0	11.1 ± 0.3	1a
DC31-100.5	DDH, -100.5 ft, Dixie Comstock mine	Whole rock (sericitized gabbro)	2.11	4.1378×10^{-11}	60.0	13.6 ± 0.4	2
DC28-285	DDH, -285 ft, Dixie Comstock mine	Calcite (stage 3)		$^{234}\text{U}/^{238}\text{U} = 2.31 \pm 1.024$ $^{230}\text{Th}/^{234}\text{U} = 1.744 \pm 0.724$ $^{230}\text{Th}/^{232}\text{Th} = 12.2 \pm 4.5$		>0.35	1b

Sources: 1a, this paper, E.H. McKee, analyst, U.S. Geological Survey, Menlo Park, CA; 1b, this paper, H.P. Schwarcz, analyst, McMaster University, Hamilton, Ontario; 2, Russell et al. (1989)
DDH = diamond drill hole

age for altered gabbro near the Dixie Comstock mine (Table 1, sample DC29-193) indicates either several intrusive events or resetting by hydrothermal fluids.

Tertiary rocks, exposed south and north of the mine (Fig. 2; Hudson and Geissman, 1987; VanLandingham, 1988), consist mainly of ash-flow tuffs interbedded with lacustrine sedimentary rocks. These rocks occur in downfaulted blocks within and adjacent to the Humboldt lopolith and are probably late Oligocene to early Miocene (Speed, 1976; Hudson and Geissman, 1987). Paleomagnetic data and geologic mapping around White Rock Canyon (Fig. 2) indicate that the Tertiary rocks and underlying gabbro were rotated 25° counterclockwise during deposition of the ash-flow tuffs (Hudson and Geissman, 1987, 1991). Rotation was largely accomplished by right-lateral strike-slip movement on northwest-trending faults, although high-angle faulting also took place (Hudson and Geissman, 1987, 1991). The rotation did not affect basalts in the Stillwater Range that date at 17 to 13 Ma (Nosker, 1981), thus limiting the onset of high-angle, normal faulting that controls present topography to post-middle Miocene.

As exposed in mine workings and drill holes, colluvium of Dixie Valley consists of several tens of feet of weakly consolidated fan deposits and lacustrine sediments overlying poorly indurated, tuffaceous sediments (Fig. 3). Fan deposits consist of irregular lenses of quartz and feldspar sand, and irregularly oriented and sized cobbles of gabbro and subordinate Tertiary volcanic rocks. Adjacent to the Dixie Comstock mine, multisized, partially aligned clasts of mineralized quartz breccia occur within fan deposits and

lacustrine and tuffaceous sediments exposed in the mine trench (Fig. 3), locally imparting ore grades to the sediments. Lacustrine sediments apparently correlate with beach gravels recognized in trenches near IXL Canyon, 15 mi southwest from the Dixie Comstock mine. These shoreline sediments were deposited by 12-ka pluvial lakes (Mifflin and Wheat, 1979; Bell and Katzer, 1990). One mile east of the mine colluvium is overlain by an ephemeral playa lake.

Quartz breccia and silica-rich clasts in trench colluvium are vertically zoned. Quartz breccia clasts are largely confined to fan deposits, lacustrine sediments, and green colluvium (Fig. 3C and D), and their abundance decreases downsection. Sparse, irregular blocks of chalcedonic silica with pockets of clay occur in the underlying green and white tuffs. Root and grass casts are present in green tuff and in chalcedonic silica clasts in white tuff, both in place and on the mine trench dump. This zonation is the inverse of silica stratigraphy that would be expected in a near-surface hydrothermal system where fossil-bearing sinter consisting of less dense and porous, un-ordered silica overlies compact quartz veins and replacement.

Alternatively, plant cast-sinter may have been derived from a younger, cospatial hydrothermal event because mine trench sediments below fan deposits are hydrothermally altered. Iron and manganese oxides encrust pebble and sand grains of lacustrine sediments, and the fine-grained matrix components of green tuff and white tuff (Fig. 3C and D) consist of poorly crystalline silica and phases amorphous to X-rays. Alteration of hanging-wall surface deposits sug-

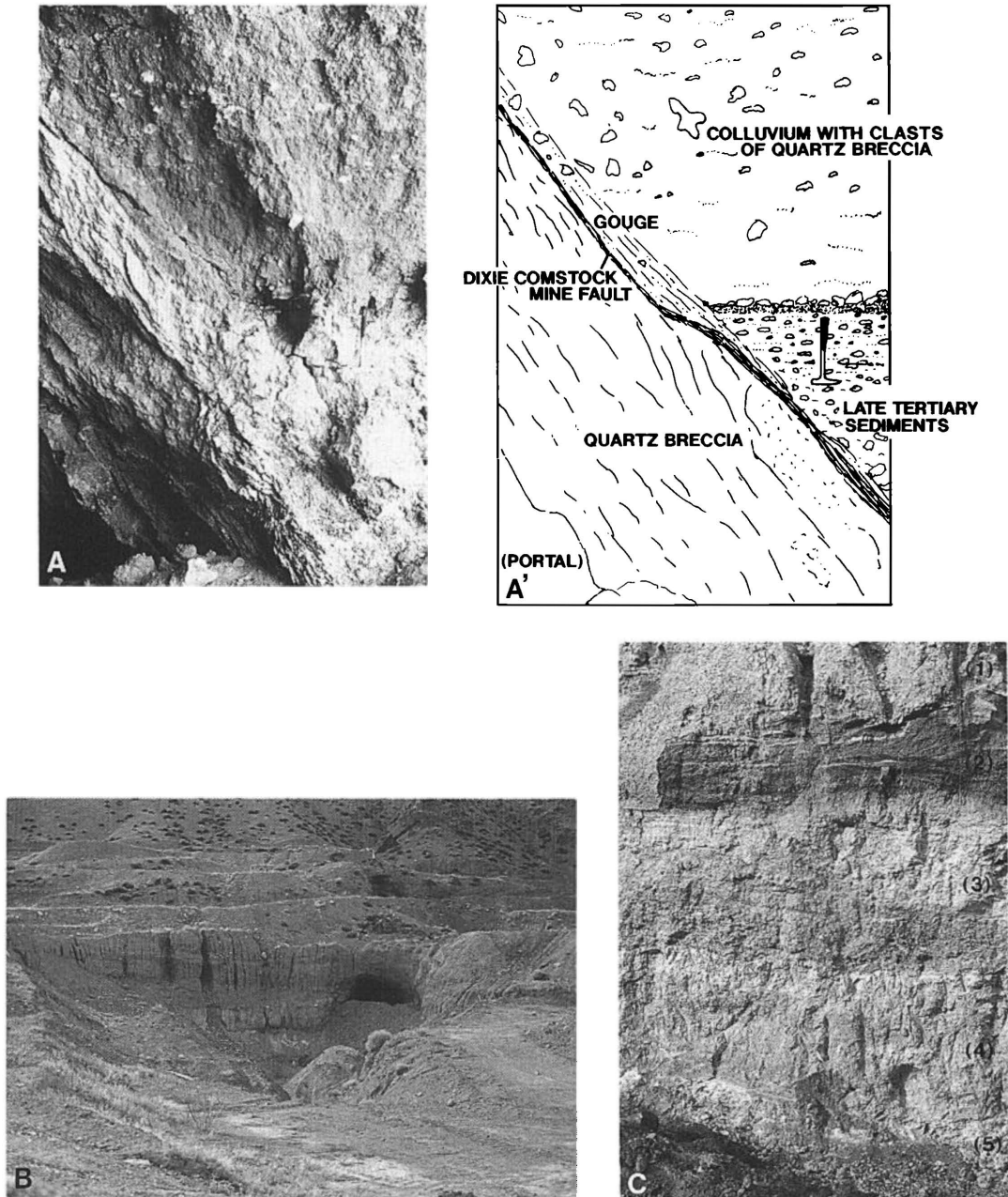


FIG. 3. A. Photograph and line drawing of the Dixie Comstock mine fault zone exposed in mine workings, with hammer for scale. Top edge of photograph is about 30 ft below the premine surface. B. Dixie Comstock mine trench created by excavation of approximately 15,000 yd³ of postmineralization, hanging-wall colluvial deposits in the 1970s. View is toward the west. Portal (right center) is the 45-ft level of the mine. White claim post (arrow, top right center) is on the apex of the quartz breccia. C. North wall of the trench showing hanging-wall stratigraphy, with knife for scale. Stratigraphy from top to bottom is (1) fan deposits, (2) lacustrine sediments, (3) green colluvium, (4) green tuff, and (5) white tuff.

gests that hydrothermal circulation in the Dixie Comstock mine fault zone resumed after partial erosion of quartz breccia, approximately coinciding with deposition of lacustrine sediments. A geothermal exploration well (DF 45-14), collared 2,500 ft southeast from the Dixie Comstock mine (Fig. 2), encountered

up to 270°F water 5,400 ft below the surface (Bell et al., 1980). In 1983, effluent from a pressure drain was depositing sulfide-rich precipitate that contained 27 ppb Au, 1.2 ppm Ag, 126 ppm As, and 58 ppm Hg. Cuttings of colluvium and volcanic rocks from the hole also contain anomalous concentrations of

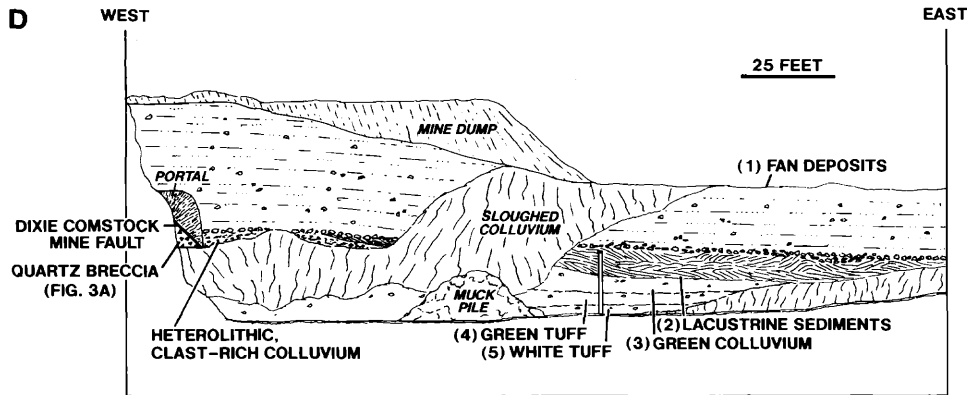


FIG. 3. D. Sketch of the north wall of the mine trench. All colluvial deposits contain angular clasts of quartz breccia or chalcedonic silica. A 0.5- to 1-ft-thick layer of quartz breccia cobbles lies on the lacustrine sediments. (1) Fan deposits—weakly indurated, partly sorted and bedded, heterolithic cobbles, sand and silt, dipping several degrees east. (2) Lacustrine sediments—weakly indurated pebbles, coarse sand and silt; heterolithic but largely gabbro clasts; finely laminated beds, abundant crossbedding; 1 to 5 percent $\text{FeO}_x + \text{MnO}_x$ encrust clasts and grains. (3) Green colluvium—infrequent, unsorted, angular cobbles of quartz breccia in an olive-green to brown silty matrix, composed mainly of comminuted gabbro detritus. (4) Green tuff—infrequent, unsorted angular cobbles of quartz breccia and chalcedonic silica in a light green silt and clay matrix with local zones of plant fragments and roots replaced by friable microcrystalline silica. (5) White tuff—rare unsorted angular and irregularly shaped blocks of chalcedonic silica containing plant fragment casts in a light green to white clay matrix.

these elements. Well temperatures, precipitate, cuttings, and altered colluvium provide evidence that metal-bearing hydrothermal fluids have been intermittently present in the Dixie Comstock mine fault zone during the Quaternary.

The age of tuffaceous sediments in the mine trench, although greater than 12 ka (Chadwick et al., 1984; Bell and Katzer, 1990), is problematic. Conformable deposition of all pre-trench sediments suggests that the tuffs are late Holocene, but no Quaternary volcanic deposits are known in the area. Exotic tephtras, reworked and thickened in the late Holocene pluvial climate (Mifflin and Wheat, 1979), are a possible source.

Dixie Comstock Mine Fault Zone

The portion of the Dixie Comstock mine fault zone which contains gold is up to 250 (76 m) ft thick, strikes north-south to $\text{N } 10^\circ \text{ E}$, and dips 40° to 45° east. It is exposed in mine workings and drainages north and south of the mine. Contiguous ore-grade gold within the fault zone forms a mullion that measures approximately 900 ft long (down-rake) by 300 ft wide by 20 to 90 ft thick and plunges 20° to 40° northeast. The apex of the mullion occurs in the mine workings where upper parts of it were locally stoped (Fig. 3B). The fault zone is composed of subparallel zones of gouge, matrix-supported quartz breccia and quartz stockwork, and along the footwall contact, incipiently crushed gabbro (Fig. 4). It may be slightly

offset by steeper piedmont faults that parallel the Stillwater Range margin (Fig. 2).

In diamond drill core, unoxidized gouge is gray to green in color, foliated parallel to contacts and composed of silt to clay-sized montmorillonite, sericite, kaolinite, feldspar, and minor pyrite. It occurs mainly along or near the hanging-wall contact and is essentially pulverized, altered gabbro. Gouge and crushed hanging-wall gabbro are included together in Figure 4.

Based on examination of drill core and mine workings, fragments in matrix-supported quartz breccia vary from angular to rounded gabbro with preserved texture to gabbro replaced by up to 100 percent quartz, minor pyrite, and other sulfides. The clasts are as much as several ft in maximum dimension but average several inches. Matrix makes up 50 to 75 percent of the breccia and consists of several generations of fine-grained to microcrystalline quartz, <1 percent pyrite, minor silicates, and vug-filling calcite. Much of the gold, especially that grading >0.2 oz Au/ton, occurs in quartz breccia. With increasing depth into the footwall, the matrix to clast ratio decreases and quartz breccia grades into stockwork.

Examination of quartz breccia in an ore stock pile and on the trench dump reveals several other textures. Some matrix consists of massive to finely banded white or mottled white-gray (from fine-grained pyrite) microcrystalline quartz that may be silicified sediment. Thin (≤ 1 mm) concentric layers of semiclear to dark gray quartz enclose clasts in

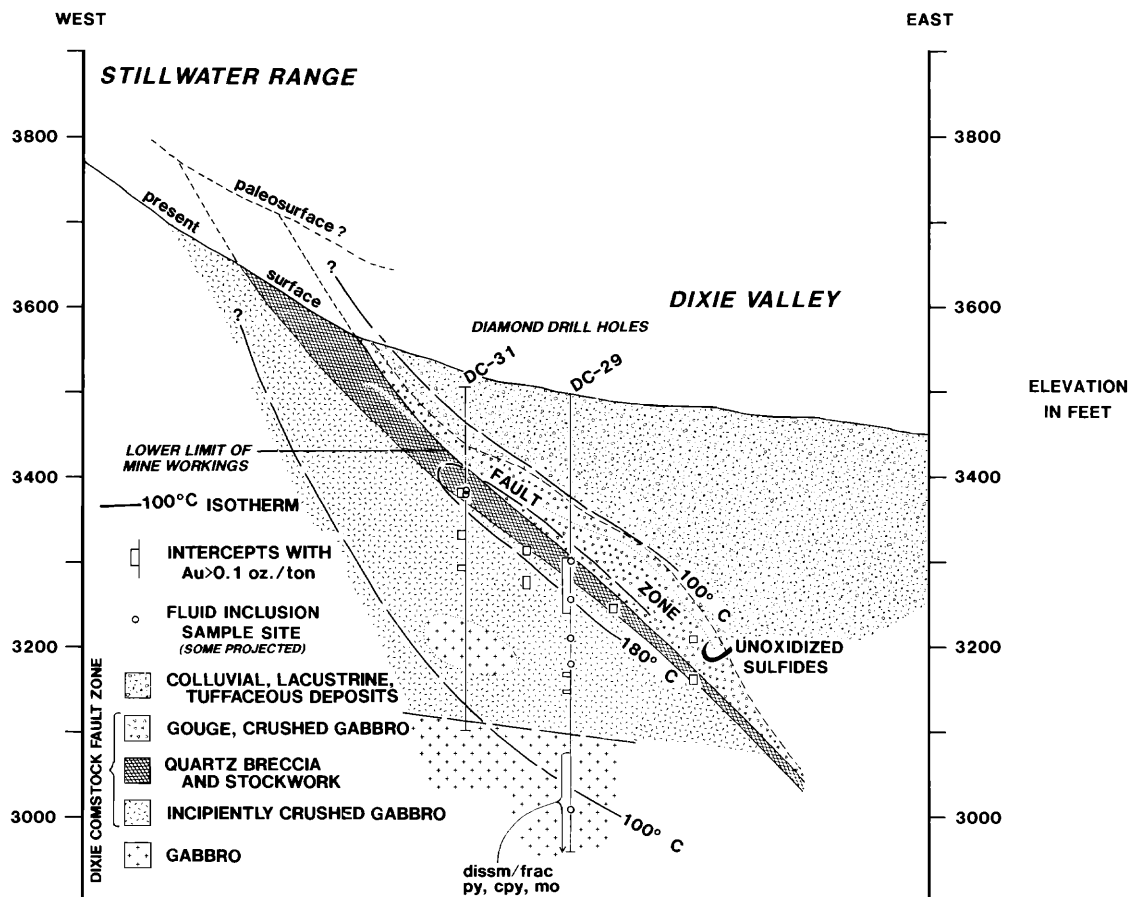


FIG. 4. West-east section through the Dixie Comstock mine and fault zone showing hanging-wall colluvium, gouge, quartz breccia and stockwork, incipiently crushed gabbro, gabbro, and higher grade gold intercepts in drill holes. Isotherms and proposed paleosurface are based on fluid inclusion microthermometry of diamond drill core and underground samples. Abbreviations: cpy = chalcopyrite, dissm = disseminated, frac = fracture, mo = molybdenite, py = pyrite.

some samples. Small clasts in other samples are well rounded and moderately well sorted. Irregular, thin crusts of opaline silica cover some quartz breccia surfaces.

Most quartz breccia is dense, extremely hard, and only occasionally vuggy. Triangular spurs along the Stillwater scarp north and south of the mine are covered by several tens of feet of quartz breccia and owe their preservation to the resistant quartz-rich matrix (Fig. 2).

Light green, soft, incipiently crushed gabbro lies along the footwall contact. It is up to 225 ft thick and in cored drill holes is in sharp contact with uncrushed footwall gabbro to the west and at depth. Incipiently crushed gabbro locally attains ore grade and makes up over 50 percent of the gold inventory. It consists of disaggregated anorthite and pyroxene grains loosely lithified by irregular (<1/8 in; <0.32 cm) seams of chlorite, minor montmorillonite, and seri-

cite, essentially forming a weakly compacted breccia, with a low matrix to clast ratio. The seams are randomly oriented and their abundance varies with no discernible pattern. Other minerals present are calcite, quartz in thin (<0.5 in) veins, titanium oxides, magnetite, coarse-grained pyrite, and molybdenite. Vuggy calcite veins up to 5 in wide cut crushed gabbro.

Gabbro beneath incipiently crushed gabbro consists of several igneous phases: (a) coarse-grained hypidiomorphic-granular anorthite and pyroxene, (b) holocrystalline, intergranular basalt intrusive into (a), and (c) segregations of zoned, automorphic feldspar crystals. Pyroxene is partially altered to chlorite, and 0.5 to 1.0 percent coarse-grained, disseminated pyrite is invariably present.

Gold (in electrum) occurs as discrete grains in quartz that cements matrix-supported breccia, and with quartz, pyrite, and chalcopyrite in breccia frag-

ments (Fig. 5). Lesser amounts of gold occur intermittently in incipiently crushed gabbro and locally attain grades exceeding 0.1 oz/ton, even where no silica is present. Assays suggest that minor amounts of electrum are also entrained in gouge. Late vuggy and vein calcite contains no electrum or sulfides.

Heavy mineral concentrates from two 5-ft drill intervals in incipiently crushed gabbro that grade >0.05 oz/ton gold consist predominantly of disseminated and narrow-vein pyrite that is unassociated with silica. These intervals are 90 to 125 ft below the quartz breccia that constitutes the higher grade portion of the gold inventory. Gold in the concentrates occurs as discrete grains of electrum and in electrum-chalcopyrite intergrowths, similar to the gold occurrences within the overlying quartz breccia (Fig. 5).

Several other sulfides occur sparingly in the deposit. Molybdenite coats fractures and is disseminated in gabbro in deeper parts of core holes. Disseminated molybdenite and pyrite in gabbro may be considerably older than other hydrothermal phases. Cinnabar thinly encrusts fracture surfaces of some underground quartz breccia samples and occurs as local concentrations in clasts within tuffaceous sediments on the trench dump. Sulfides in all three components of the fault zone are largely unoxidized, and iron oxides occur only within several tens of feet of the surface.

Within quartz breccia and stockwork in drill core are local zones of sericitized gabbro that have not been completely brecciated and replaced by quartz. Sericite from several of these zones has K-Ar ages of 15.0, 11.1, and 13.6 Ma (Table 1, samples DC-29-208.5, DC-29-210, and DC-31-100.5). Fluid inclusion homogenization temperatures and fault displacement rate data presented later indicate that sericite

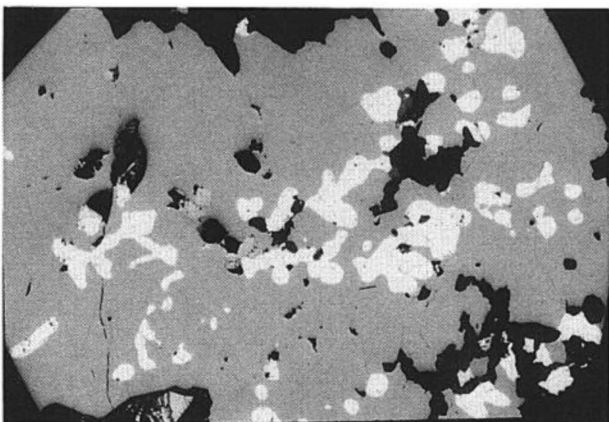


FIG. 5. Microphotograph of electrum (light, reflective inclusions) in chalcopyrite in an underground sample from the Dixie Comstock mine. Electrum in this sample consists of ~53 wt percent Au and 47 wt percent Ag. Width of frame is approximately 0.6 mm.

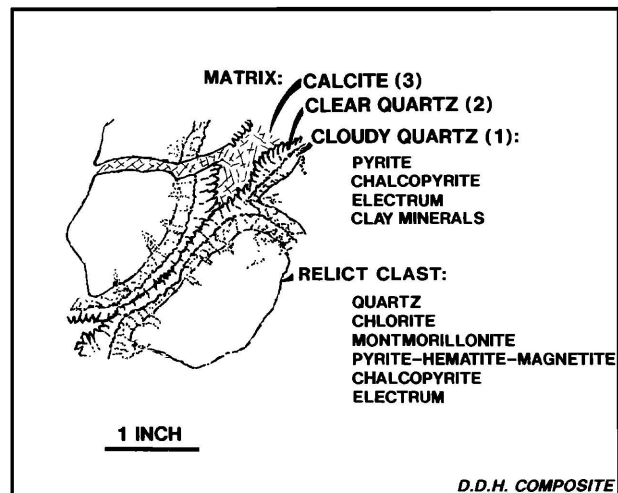


FIG. 6. Schematic depiction of the three stages of matrix hydrothermal minerals and relict gabbro clasts, compiled from examination of diamond drill core.

predates quartz breccia and gold mineralization. Sericite ages apparently record early hydrothermal fluid circulation in the Dixie Comstock mine fault and support a post-middle Miocene age for initial Basin and Range faulting in this area. The age of gold mineralization is interpreted to be Pleistocene based on thickness of cover and erosion rates that are discussed in following sections.

Paragenesis

Three stages of hydrothermal mineralization are recognized in quartz breccia from drill core (Fig. 6). Quartz that replaced gabbro clasts contains electrum, pyrite, and minor chalcopyrite, all of which coexist with chlorite, montmorillonite, and iron oxides. Based on common minerals, this relict clast assemblage is apparently coeval with the earliest matrix, stage 1, which consists of cloudy quartz, electrum, pyrite, rare chalcopyrite, and clay minerals. Total sulfide in clasts approaches 5 vol percent whereas early matrix sulfide rarely exceeds 1 vol percent. Correspondingly, electrum is several times more abundant in replaced clasts, suggesting that alteration of pyroxene and feldspar locally controlled gold deposition. Electrum in cloudy quartz of the matrix is also appreciably more abundant in clay aggregates. Stage 1 electrum contains 55 to 61 mole percent silver (Table 2, samples DC-83-1 and DC-29-214.4). Electrum from narrow sulfide veins in incipiently crusted gabbro contains 52 to 56 mole percent silver (Table 2, samples DC-29-348-353 and DC-28-345-350) and probably correlates with the stage 1 assemblage in quartz breccia.

The second stage of mineralization consists of clear, euhedral, locally vuggy quartz, that was depos-

TABLE 2. Compositions (wt %) of Electrum in Ore-Grade Samples from the Dixie Comstock Mine

Sample no.	No. of analyses	Au	Ag	S	Sum	N _{Ag} ^{el}
DC83-1a	3	54.45	46.79	0.21	101.45	61.1
DC83-1b	2	52.20	47.50	0.25	99.95	62.4
DC29-214.4a	2	58.82	39.22	0.18	98.22	54.9
DC29-214.4b	2	58.50	39.14	0.05	99.27	55.0
DC29-348-353	1	56.58	39.86	0.22	96.66	56.3
DC28-345-350	2	62.93	37.26	0.20	100.39	51.9

Determined by electron microprobe; N_{Ag}^{el} is mole percent silver in electrum.

ited over electrum + sulfide matrix, cloudy quartz (stage 1). The contact between early matrix cloudy quartz (stage 1) and later matrix clear quartz (stage 2) is sharp. The youngest matrix mineral and third stage of mineralization is coarse-grained calcite that fills vugs in clear quartz (stage 2) or occurs as veins cutting all earlier assemblages.

Fluid Inclusion Homogenization Temperature Data

Coarse-grained hydrothermal minerals in the Dixie Comstock mine fault zone are uncommon. Only limited microthermometric measurements were made on fluid inclusions in quartz and calcite from nine drill core, drill cuttings, and underground samples. Some fluid inclusion data were also collected from barite and calcite veins up to 0.25 mi southwest of the mine.

Fluid inclusions from which data were collected are thought to be primary because they mostly occur isolated in crystal growth zones. Inclusions in all samples are liquid rich and contain no daughter minerals. Inclusions in clear quartz overgrowths (the second stage of mineralization) in several mine samples contain no vapor phase and are assumed to be entirely liquid. Inclusion size never exceeds 10 μm, and collection of accurate salinity data by freezing inclusions proved infeasible. Low homogenization temperatures and predominance of meteoric water (see later section) in inclusions suggest low fluid salinities. An average of 30 determinations was used to define each of the temperature modes cited below, which differ by no more than several degrees from median T_h. Examples of fluid inclusion microthermometric data are shown in Figure 7.

Inclusions in stage 1 cloudy quartz intergrown with pyrite, chalcopyrite, and electrum gave T_h modes of 175° to 185°C. Inclusions in several stage 1 quartz samples homogenized over a wide temperature range, displaying no clear mode (Fig. 7). Inclusions in stage 2 clear quartz homogenized at modal temperatures ranging from 170° to 210°C, although single-phase (liquid) inclusions observed in quartz of this stage undoubtedly formed at lower temperatures. Inclusions in stage 2 clear quartz usually displayed a much larger T_h range than mineralized stage 1 cloudy

quartz, and some inclusions homogenized at temperatures greater than 250°C. Inclusions in three stage 3 calcite samples homogenized to liquid, giving modes of 165°, 172°, and 176°C.

A sample of vein calcite 0.25 mi southwest of the mine gave a fluid inclusion homogenization temperature mode of 158°C. A sample of vein barite from the same location gave no clear temperature mode, having a T_h range of 140° to 200°C.

Quartz that replaced gabbro clasts cannot be clearly related in time to electrum precipitation, although quartz, electrum, sulfides, and clay minerals appear to be texturally coeval. Electrum in early matrix cloudy quartz (stage 1) is unequivocally a coprecipitant, and isotherms in Figure 4 record temperature distribution of this paragenetic stage. However, temperatures at which stage 2 clear quartz and stage 3 calcite were deposited are nearly indistinguishable from those of electrum-bearing, stage 1 quartz.

Therefore, most, if not all, electrum in quartz breccia was deposited at 175° to 180°C. Electrum in incipiently crushed gabbro may have precipitated at different temperatures, but those electrum composi-

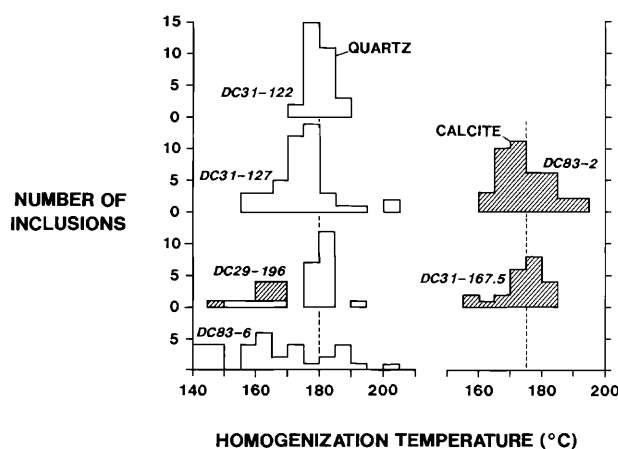


FIG. 7. Examples of fluid inclusion homogenization temperature histograms for the Dixie Comstock mine stage 1 quartz and stage 3 calcite (see Fig. 6). Data were derived from diamond drill core and underground samples. Several other samples displayed homogenization temperature variability similar to that of sample DC83-6.

tions (Table 2) and mineral associations are very similar to quartz breccia electrum. The position of the 100°C isotherm in Figure 4 is consistent with the preponderance of single-phase inclusions in deeper samples and presumed temperature buffering by water-saturated colluvium above the quartz breccia. It appears that higher fluid temperatures were largely confined to quartz breccia and stockwork and that heat was convected by fluid toward the surface, primarily in the Dixie Comstock mine fault zone.

Although little evidence for boiling was observed in drill hole samples, inclusions in quartz from surface mine workings trapped boiling fluids, as evidenced by a few coeval vapor- and liquid-rich inclusions, at slightly lower temperatures (160°–170+°C). Large homogenization temperature variability in several stage 1 samples also supports vapor-liquid separation during entrapment (Fig. 7). It is assumed that the drill hole inclusions were formed within a few degrees of boiling at 180°C and no pressure corrections have been applied to homogenization temperatures. According to pure water phase separation curves (Haas, 1971), fluids in quartz breccia in drill holes DC-31 and DC-29 circulated about 330 ft (100 m) below the surface (Fig. 4). If eroded sinter clasts are coeval with quartz breccia, then the paleosurface and water table were essentially coplanar and the thickness of eroded sinter, quartz breccia, and quartz stockwork is ≤ 330 ft (Fig. 4).

The fine grain size and fluid inclusion homogenization temperatures of $\sim 180^\circ\text{C}$ suggest that hydrothermal quartz of the quartz breccia may have originally

been deposited as chalcedony or amorphous silica. The solubility of silica in geothermal systems below 180° is usually controlled by chalcedony (Fournier, 1985). Subsequent recrystallization of chalcedony or coalescing grain growth may have produced the observed quartz breccia matrix textures and may have modified primary fluid inclusions. Recognition of a chalcedonic precursor according to the criteria of Sander and Black (1988) is not clear in the fluid inclusion samples examined, but it remains possible that homogenization temperature modes are recording the chalcedony-quartz transition and that higher silica depositional temperatures have been overlooked.

Light Stable Isotope Data

Deuterium and oxygen isotope abundances in fluid inclusions were obtained from four stage 1 cloudy quartz and two stage 3 calcite drill core samples (Table 3) for which homogenization temperatures had been determined or could be closely estimated. The $\delta\text{D}_{\text{H}_2\text{O}}$ values range from -106 to -123 per mil, and calculated $\delta^{18}\text{O}_{\text{H}_2\text{O}}$ values range from -6.7 to -14.3 per mil. Water in calcite is most depleted in deuterium and, in one sample, most enriched in ^{18}O . Analytical precision for hydrogen is ± 5 per mil and for oxygen, ± 0.5 per mil.

Isotopic compositions of deep geothermal well waters in Dixie Valley, $\delta\text{D} = \sim -101$ to -126 per mil and $\delta^{18}\text{O} = \sim -10.6$ to -14.8 per mil (Ingraham, 1982, appendix A), encompass Dixie Comstock mine quartz fluid δD and $\delta^{18}\text{O}$ values, although Dixie Comstock mine quartz fluid δD values are generally 5 to

TABLE 3. Light Stable Isotope Data for Fluid Inclusion Water in Quartz and Calcite, and for Pyrite Sulfur from Drill Holes at the Dixie Comstock Mine

Sample no.	Depth below the surface (ft)	Mineral	T ¹ (°C)	$\delta\text{D}_{\text{H}_2\text{O}}$ (‰)	$\delta^{18}\text{O}_{\text{quartz, calcite}}$ (‰)	$\delta^{18}\text{O}^2$ (‰)
DC29-214.4	-214.4 ft	Quartz	e180	-106	+0.8	-12.1
DC31-122	-122 ft	Quartz	179	-112	-1.6	-14.5
DC31-127A	-127 ft	Quartz	175	-108	-0.4	-13.6
DC31-127B	-127 ft	Quartz	175	-108	+0.1	-13.1
DC28-273	-273 ft	Calcite	e176	-116	+4.2	-6.7
DC31-167.5	-167.5 ft	Calcite	176	-123	-3.4	-14.3
Sample no.	Depth below the surface (ft)	Mineral			$\delta^{34}\text{S}$ (‰)	
DC28-228.5-231.5	-228.5 to -231.5	Pyrite			-7.5	
DC28-253-258	-253 to 258 ft	Pyrite			-6.7	
DC28-458-463	-458 to 463 ft	Pyrite			-3.5	
DC29-188-193.5	-188 to 193.5 ft	Pyrite			-7.2	
DC29-524-529	-524 to 529 ft	Pyrite			-3.0	
DC31-201.5-204	-201.5 to 204 ft	Pyrite			+3.9	

Analyses done by Geochron Laboratories (Cambridge, MA); e = estimated from fluid inclusion homogenization temperatures where no clear mode is present

¹ Determined from fluid inclusion homogenization

² Calculated using the equation: $10^3 \ln \alpha = 3.34 (10^{-6} \text{T}^{-2}) - 3.31$ for quartz-water (Matsuhisa et al., 1979) and $10^3 \ln \alpha = 2.78 (10^{-6} \text{T}^{-2}) - 2.89$ for calcite-water (Friedman and O'Neil, 1977), extrapolated to lower temperatures indicated by fluid inclusion homogenization

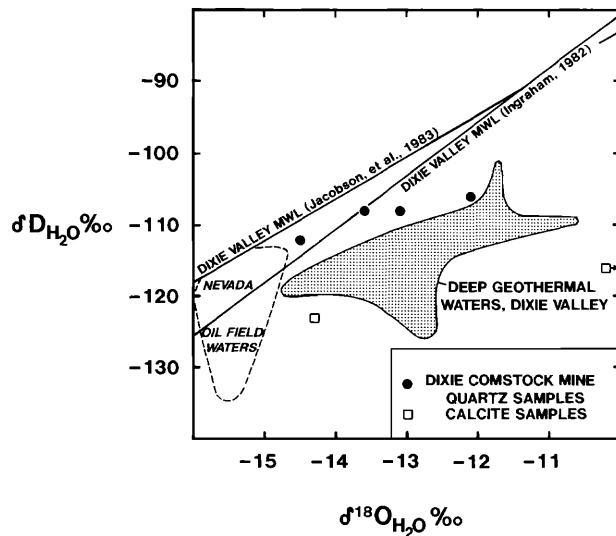


FIG. 8. Isotopic composition of stage 1 cloudy quartz fluid from diamond drill hole samples at the Dixie Comstock mine and deep geothermal waters in Dixie Valley. Nevada oil field water analyses provided by R.L. Jacobson (University of Nevada, Desert Research Institute) on water samples collected by the author and field operators.

10 per mil higher (Fig. 8). Quartz fluids and one calcite fluid composition are displaced up to several per mil from a local meteoric water line (determined by Ingraham, 1982) by water-rock oxygen exchange. Much greater exchange is indicated by a second calcite fluid isotopic composition (Fig. 8). Isotope compositional similarities show that quartz breccia meteoric water and, in part, late calcite meteoric water resemble modern deep geothermal water in Dixie Valley and that Dixie Comstock mine hydrothermal phases were deposited from nearly unexchanged meteoric water (Fig. 8).

The $\delta^{34}\text{S}$ values determined for six pyrite drill core samples range from -7.5 to +3.9 per mil (Table 3). Analyzed pyrites were derived from stage 1 quartz breccia matrix and from incipiently crushed gabbro. Five values are between -3.0 and -7.5 per mil, possibly reflecting igneous sulfur that has been isotopically depleted under low pH and/or high f_{O_2} fluid conditions that favor dissolved sulfate. It is also possible that several generations of pyrite were analyzed. The variations in sulfur isotope compositions of pyrite bear no discernible spatial relation to the Dixie Comstock mine fault nor to quartz breccia paragenesis.

The isotopic compositions of water and sulfur in the Dixie Comstock mine yield no definitive genetic information. Meteoric waters are known to circulate to many thousands of feet below the surface in Great Basin geothermal fields (Ingraham, 1982; Jacobson et al., 1983) and oil fields (Fig. 8). Furthermore,

hundreds of feet of water-saturated colluvium in Dixie Valley provide an immense fluid reservoir and nearly unlimited access to hydrothermal components for shallow mineralization.

Faulting History

Three epochs of faulting are recognized along the eastern margin of the Stillwater Range from White Rock Canyon to south of the Dixie Comstock mine: Oligocene-Miocene, middle Miocene, and Quaternary.

Late Oligocene-early Miocene rotational faulting, identified from paleomagnetic and fault-slip data on ash-flow tuffs and lacustrine rocks dated at 32 to 22 Ma, was concurrent with deposition of the ash-flow tuffs (Hudson and Geissman, 1987). Rotational faults are thought to predate 17 to 13 Ma basalts in the Stillwater Range that are relatively undeformed and flat lying.

Oligocene-Miocene volcanic rocks are also displaced by normal faults that dip 35° to 60° east. These faults were active during the second epoch, which includes the Dixie Comstock mine fault. They were active by the middle Miocene (Fig. 2), since sericitized gabbro samples in the Dixie Comstock mine fault have K-Ar ages that range from 15.0 to 11.1 Ma (Table 1). In the area of Figure 2, the Dixie Comstock mine fault consists of several curvilinear segments, 0.5 to 2 mi long, which separate Mesozoic from Tertiary rocks, Mesozoic and Tertiary rocks from colluvium of Dixie Valley, and older terrace gravel deposits from colluvium. Based on geothermal well logs (Bell et al., 1980), middle Miocene-initiated faults cumulatively displaced Mesozoic and Tertiary rocks of the Stillwater Range for thousands of feet (Fig. 9) and created an ancestral Dixie Valley.

Pleistocene-Holocene normal faults, the third epoch, are largely parallel to or coplanar with middle Miocene faults along the present range margin. In the Dixie Comstock mine, they manifest as hanging-wall gouge and crushed gabbro above quartz breccia and may include the quartz breccia also. North and south of the mine Quaternary faults displace fan deposits as well as Tertiary volcanic rocks from colluvium of Dixie Valley (Fig. 2) and are thought to be as young as 10,000 yr (Wallace and Whitney, 1984). At the Dixie Comstock mine, clasts of quartz breccia and chalcedonic silica occur in hanging-wall Holocene colluvial deposits (Fig. 3), providing evidence that the quartz breccia was exposed by Quaternary fault displacements.

Piedmont faults, recognized from geophysical data and low-sun-angle photography, are also considered to have originated in the Quaternary, based on scarp examination near IXL Canyon, 15 mi southwest of the Dixie Comstock mine (Bell and Katzer, 1987, 1990). Movement on piedmont faults there has both

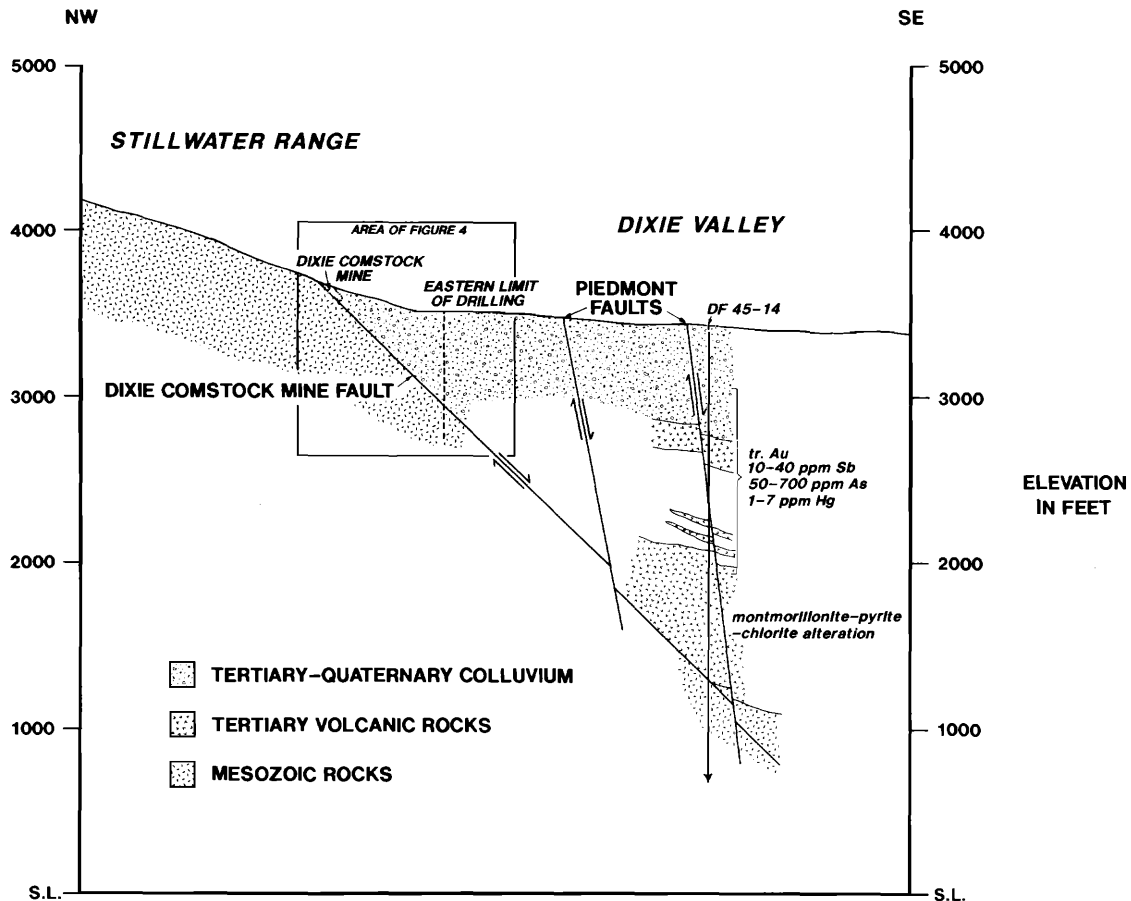


FIG. 9. Northwest-southeast section through the Dixie Comstock mine and geothermal well DF 45-14 showing projected structure and stratigraphy. Anomalous Au, Sb, As, and Hg in intercalated colluvium and volcanic rocks suggests intermittent Quaternary hydrothermal activity.

alternated and coincided with range-bounding fault displacement during the Holocene. In the vicinity of the Dixie Comstock mine, piedmont faults are hundreds to thousands of feet east of the range margin (Fig. 2) and may downdrop quartz breccia and Tertiary volcanic rocks to the east (Figs. 2 and 9). Their dip would, therefore, exceed 45° .

Some constraints on the age of quartz breccia gold mineralization can be derived from extrapolation of current fault displacement rates and from the amount of eroded premineralization cover. Two assumptions must be made:

1. Quartz breccia is not displaced relative to footwall gabbro, thus providing a footwall datum. Because Holocene postmineralization gouge and crushed gabbro within the fault zone are along the hanging-wall contact above the quartz breccia, this requirement is apparently satisfied, although cumulative postmineralization movement within incipiently crushed gabbro in the footwall beneath quartz breccia could be appreciable. If quartz breccia did

not remain fused to footwall gabbro, the estimated age is minimum.

2. The thickness of cover at the time of mineralization can be accurately determined from quartz breccia fluid inclusion data. The depositional temperature of Dixie Comstock mine quartz breccia is approximately 180°C , giving a minimum thickness of premineralization cover of about 330 ft (100 m). Relatively shallow cover during and limited erosion after mineralization are supported by sinter clasts in hanging-wall colluvium.

Quaternary fault displacement timing and rates in Dixie Valley of ~ 0.3 to 0.5 mm/yr (Wallace and Whitney, 1984; Okaya and Thompson, 1985; Bell and Katzer, 1990) correlate with accelerated extension (Thompson and Burke, 1973) and suggest that most displacement along the eastern Stillwater Range margin has taken place during the last few million years. At an average Holocene displacement rate of 0.4 mm/yr, approximately 0.25 Ma of uplift (and erosion) are required for the present level of quartz

breccia exposure. This relatively young age for quartz breccia gold mineralization is supported by the similarity in isotopic compositions of Dixie Comstock mine quartz fluid and modern deep geothermal waters from Dixie Valley (Fig. 8) as well as by colluvial stratigraphy.

A uranium-thorium age of >0.35 Ma, determined for stage 3 calcite from drill core (Table 1), suggests a mineralization age somewhat older than that estimated from present fault displacement rates. Thus, erosion of estimated postmineralization cover (~ 330 ft; 100 m) may have begun by the middle Pleistocene. Although one calcite radiometric age is not necessarily definitive and fluid inclusion temperatures are somewhat imprecise, both data imply intermittently lower average fault displacement rates in the Pleistocene. If gold mineralization is as old as 0.5 Ma, approximately 660 ft of postmineralization cover would have been removed at present fault displacement rates, requiring significantly higher depositional temperatures (up to 210°C) than measured. Therefore, "seismic gaps," "displacement grouping" (Wallace and Whitney, 1984; Wallace, 1987), or temporal clustering of displacement along Dixie Valley range margin faults may be as old as middle Pleistocene.

Conclusions

Age, temperature, and stratigraphic data obtained from hydrothermal minerals deposited in the Dixie Comstock mine fault, which separates the Stillwater Range from Dixie Valley, indicate that: (1) displacement along this range-bounding fault began at least by the middle Miocene, (2) of the several hydrothermal events which utilized the fault, a mid-Pleistocene event deposited potentially bulk mineable gold in a million, (3) gold mineralization took place at $\sim 180^{\circ}\text{C}$ beneath ~ 330 ft (~ 100 m) of cover, (4) gold and associated quartz, sulfides, silicates, and calcite were precipitated from heated ground water, and (5) the present pattern of spatial and temporal clustering of fault displacements in Dixie Valley is apparently mid-Pleistocene or older.

Acknowledgments

Appreciation is extended to ASARCO Incorporated for sponsoring this research and its publication. Ted McKee graciously provided three K-Ar ages which helped to order igneous and hydrothermal events. The comments of two *Economic Geology* reviewers significantly improved clarity of the paper.

June 2, November 18, 1993

REFERENCES

- Bell, E.J., Campana, M.E., Jacobsen, R.L., Larson, L.T., Slemmons, D.B., Bard, T.R., Bohm, B.W., Ingraham, N.L., Jucal, R.W., and Whitney, R.A., 1980, Geothermal reservoir case study, northern Basin and Range province, northern Dixie Valley, Report: Reno, University of Nevada, Mackay Mineralogical Research Institute, 233 p.
- Bell, J.W., and Katzer, T., 1987, Surficial geology, hydrology, and late Quaternary tectonics of the IXL Canyon area, Nevada, as related to the 1954 Dixie Valley earthquake: Nevada Bureau of Mines and Geology Bulletin 102, 52 p.
- 1990, Timing of late Quaternary faulting in the 1954 Dixie Valley earthquake area, central Nevada: *Geology*, v. 18, p. 622–625.
- Chadwick, O.A., Hecker, S., and Fonseca, J., 1984, A soils chronosequence at Terrace Creek: Studies of late Quaternary tectonism in Dixie Valley, Nevada: U.S. Geological Survey Open-File Report 84–90, 29 p.
- Fournier, R.O., 1985, The behavior of silica in hydrothermal solutions: *Reviews in Economic Geology*, v. 2, p. 45–59.
- Friedman, I., and O'Neil, J.R., 1977, Compilation of stable isotope fractionation factors of geochemical interest: U.S. Geological Survey Professional Paper 440 KK, 12 p.
- Haas, J.L., 1971, The effect of salinity on the maximum thermal gradient of a hydrothermal system at hydrostatic pressure: *ECONOMIC GEOLOGY*, v. 66, p. 940–946.
- Hudson, M.R., and Geissman, J.W., 1987, Paleomagnetic and structural evidence for middle Tertiary counterclockwise block rotation in the Dixie Valley region, west central Nevada: *Geology*, v. 15, p. 638–642.
- 1991, Paleomagnetic evidence for the age and extent of middle Tertiary counterclockwise rotation, Dixie Valley region, west-central Nevada: *Journal of Geophysical Research*, v. 96, p. 3979–4006.
- Ingraham, N.L., 1982, Environmental isotope hydrology of the Dixie Valley geothermal system, Dixie Valley, Nevada: Unpublished M.S. thesis, Reno, University of Nevada, 96 p.
- Jacobson, R.L., Ingraham, N.L., and Campana, M.E., 1983, Isotope hydrology of a Basin and Range geothermal system: University of Nevada, Reno, Desert Research Institute, Publication 41087, 18 p.
- Matsuhisa, Y., Goldsmith, J.R., and Clayton, R.N., 1979, Oxygen isotopic fractionation in the system quartz-albite-anorthite-water: *Geochimica et Cosmochimica Acta*, v. 43, p. 1131–1140.
- Mifflin, M.D., and Wheat, M.M., 1979, Pluvial lakes and estimated pluvial climates of Nevada: Nevada Bureau of Mines and Geology Bulletin 94, 57 p.
- Nosker, S.A., 1981, Stratigraphy and structure of the Sou Hills, Pershing County, Nevada: Unpublished M.S. thesis, Reno, University of Nevada, 60 p.
- Okaya, D.A., and Thompson, G.A., 1985, Geometry of Cenozoic extensional faulting: Dixie Valley, Nevada: *Tectonics*, v. 4, p. 107–125.
- Oldow, J.S., 1992, Late Cenozoic displacement partitioning in the northwestern Great Basin: Walker Lane Symposium, Geological Society of Nevada, Reno, NV, 1992, Proceedings, p. 17–52.
- Page, B.M., 1965, Preliminary geologic map of a part of the Stillwater Range, Churchill County, Nevada: Nevada Bureau of Mines and Geology, Map 28, scale 1:250,000.
- Parry, W.T., Hedderly-Smith, D., and Bruhn, R.L., 1991, Fluid inclusions and hydrothermal alteration on the Dixie Valley fault, Nevada: *Journal of Geophysical Research*, v. 96, p. 19,733–19,748.
- Sander, M.V., and Black, J.E., 1988, Crystallization and recrystallization of growth-zoned vein quartz crystals from epithermal systems—implications for fluid inclusion studies: *ECONOMIC GEOLOGY*, v. 83, p. 1052–1060.

- Slemmons, D.B., and Bell, J.W., 1987, 1954 Fairview Peak earthquake area, Nevada: Boulder, Colorado, Geological Society of America, Centennial Field Guide, v. 1, p. 73-76.
- Speed, R.C., 1976, Geologic map of the Humboldt lopolith and surrounding terrain, Nevada: Geological Society of America Map MC-14, scale ~1:80,000.
- Thompson, G.A., and Burke, D.B., 1973, Rate and direction of spreading in Dixie Valley, Basin and Range province, Nevada: Geological Society of America Bulletin, v. 84, p. 627-632.
- Vanderburg, W.O., 1940, Reconnaissance of mining districts in Churchill County, Nevada: U.S. Bureau of Mines Information Circular 7093, p. 48.
- VanLandingham, S.L., 1988, Comment and reply on "Paleomagnetic and structural evidence for middle Tertiary counterclockwise block rotation in the Dixie Valley region, west-central Nevada": *Geology*, v. 16, p. 756-757.
- Waibel, A.F., 1987, An overview of the geology and secondary mineralogy of the high temperature geothermal system in Dixie Valley, Nevada: Geothermal Resources Council Bulletin, Sept/Oct., v. 16, p. 5-11.
- Wallace, R.E., 1984, Patterns and timing of late Quaternary faulting in the Great Basin province and relation to some regional tectonic features: *Journal of Geophysical Research*, v. 89, p. 5763-5769.
- 1987, Grouping and migration of surface faulting and variations in slip rates on faults in the Great Basin province: *Seismological Society of America Bulletin*, v. 77, p. 868-876.
- Wallace, R.E. and Whitney, R.A., 1984, Late Quaternary history of the Stillwater seismic gap, Nevada: *Seismological Society of America Bulletin*, v. 79, p. 301-314.
- Willden, R., and Speed, R.C., 1974, Geology and mineral deposits of Churchill County, Nevada: Nevada Bureau of Mines and Geology Bulletin 83, 95 p.